

THE HIGH PERFORMANCES OF A SEVEN LEVELS ACTIVE POWER FILTER WITH A FUZZY LOGIC CONTROLLER UNDER A HIGH VOLTAGE

M. S. DJEBBAR^{1,*}, H. BENALLA²

¹Faculty of Engineering Sciences, on Electrical Laboratory,
University of Tebessa, Constantine Road, Tebessa12002, Algeria

²University Mentouri brothers, Constantine1, Faculty of science technology
Electrical Engineering Department, Algeria

*Corresponding Author: djebbarn@yahoo.fr

Abstract

This paper proposes a new perspective in the contribution to the purifying of harmful harmonics in the electric power distribution network. This perspective consists of using a seven-level parallel active filter that reveals superior qualities to those of the conventional two-level active filter. The three-phase seven-level inverter is equipped with a fuzzy controller, designed to keep the DC bus voltage constant. In order to effectively compensate the disturbances responsible of the performance degradation of the electrical equipment, the active filtering is treated according to an approach based on the use of the instantaneous active and reactive power method. Consequently the power factor unity, the sine wave current source and the minimal reactive power will be improved. The control strategy used to command the inverter switches is the intersective six-carrier *PWM*. These latter offers to the filtering operation a high stability and robustness in the various perturbations proposed in this work. The performed robustness tests clearly show the efficiency and the stability of the adopted approach for the *SAPF*, and this justifies the use of this type of filter in the field of high voltage and great power such as electrical traction.

Keywords: Fuzzy controller, Shunt active power filter (*SAPF*), Theory (*p-q*).

1. Introduction

Recent developments in the power electronics industry have led to considerable power growth that can be handled by semiconductor devices. However, the maximum voltage supported by these devices remains the major obstacle in high and medium voltage applications. In order to remedy the limitations of the switches

Nomenclatures

F	Connections functions
F_k^b	Half-arm connection functions
$I_{f inj}$	Harmonic current filter injected, A
I_{ha}	Harmonic current for phase (a), A
I_f^*	Harmonic current filter reference, A
I_s	Current source, A
M	Modulation index
p	Instantaneous active power, W
q	Instantaneous reactive power, VAR
r	Modulation rate
V_f	Voltage filter, V

Greek Symbols

α	Phase α , concordia direct transformation
β	Phase β , concordia direct transformation

Abbreviations

CDT	Concordia Direct Transformation
DC	Direct Current
FLC	Fuzzy Logic Controller
LPF	Low-Pass Filters
SAPF	Shunt Active Power Filter
SPWM	Sinusoidal Pulse Width Modulation

inverse voltages, several new techniques and topologies have been developed. For example: Multiple H-bridge Converter, Flying Capacitor Converter, Neutral Point Clamped structure (*NPC*) and Multiple Point Clamped structure (*MPC*) [1- 4]. These converters are suitable for high voltage and high power applications because of their ability to synthesize waveforms with better harmonic spectra and reach high voltages with a limited maximum frequency of the devices [5]. These qualities of the multi-level inverter have led to the idea of using a parallel active filter that consists of a seven-level voltage inverter.

This latter will contribute to the minimization of the harmonics occurring in the electric power distribution networks caused by the connection to non-linear loads (the most common are electronic motor starters, electronic speed controllers, and other electronic devices, welding stations and uninterruptible power supplies (*UPS*)). Harmonic distortion is a form of power grid pollution that can create anomalies (heating of transformers, cables, motors, generators and capacitors, possible tripping of circuit breakers, malfunctioning of computers ...). This will occur when the sum of the harmonic currents exceeds certain limit values [6]. The adopted method to reduce these disturbances must take into account three major factors: the load, the power supply and the allowed level of distortion. In fact, the main role of active filtering, whatever its structure (two or multilevel), is to control the harmonic distortion in an active way, and this is done by the compensation of the existing harmonics in the electrical network at any moment in time.

This operation is carried out by generating harmonic currents equal in amplitude and opposite in phase with those produced by the polluting loads [7] as shown in the following Fig. 1. The *FAP* studied in this work is based on the identification of harmonic currents under the principle of calculating the instantaneous active and reactive power [8, 9]. This has allowed us to have a clear improvement in the quality of the electrical energy, even in the case of the various disturbances created during the numerical simulations.

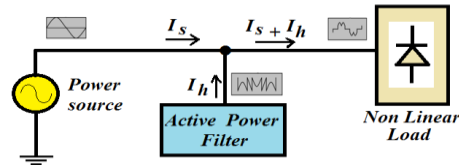


Fig. 1. Principle of shunt active power filter (Shunt APF).

The Shunt Active Power Filter (Shunt *APF*) consists of generating harmonics in opposition to those that are existing in the network (as shown in Fig. 2). This operation causes a sinusoidal absorption in the electrical network. The current absorbed by the pollutant load remains non-sinusoidal.

The objective of this work is to implement a seven levels shunt *APF* under different perturbations and to evaluate the performance of the filter in a medium voltage network. The Shunt *APF* is a voltage inverter that compensates harmonic currents, as shown in Fig. 2, the shunt is connected to the pollutant load. It consists of two parts, the power part and the control part. The power section is constituted by a seven level voltage inverter power based switches, controllable at the opening and the closure in anti-parallel with the diodes. It has also an energy storage circuit, often capacitive (six capacitors), and an input filter L_f .

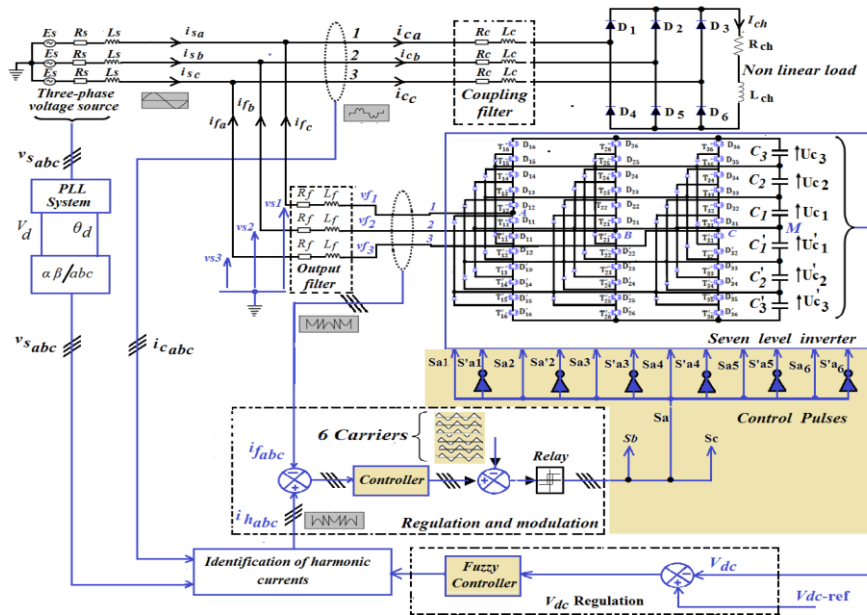


Fig. 2. Seven level active power filter block diagram.

2. Modeling and Control

2.1. Seven level inverter modeling

The three-phase voltage inverter allows us to obtain seven voltage levels at its output (refer Table 1), its structure is illustrated by the Fig. 3.

The complementary control retained [10, 11] is characterized by a relationship between the connection functions of the switches of an arm k as follows Eq. (1):

$$F'_{ki} = 1 - F_{k(7-i)}, \quad i = 1, \dots, 6 \text{ and } k = 1, 2, 3 \quad (1)$$

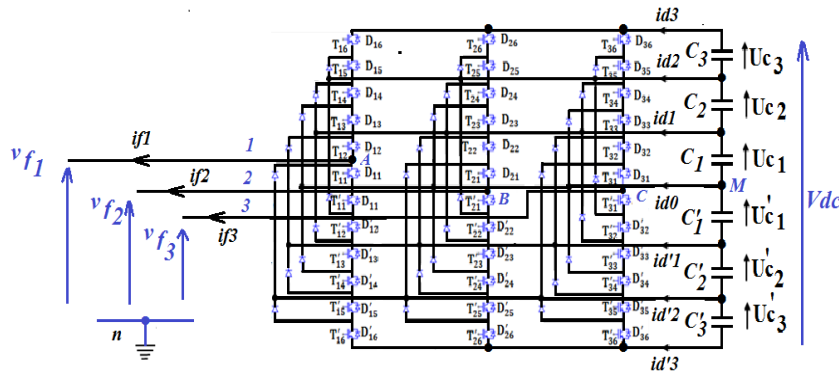


Fig. 3. Three phase seven level inverter structure of a diode clamped.

The possible states of an arm k while taking account of the complementary control selected are given in Table 1. State 1 means that the corresponding switch is closed and state 0 means it is open. This table shows that this complementary control gives us the possibility of exploiting the seven voltage levels in the output for an arm of the inverter.

Table 1. States the seven level inverter and output voltage V_{kM} .

F_{k1}	F_{k2}	F_{k3}	F_{k4}	F_{k5}	F_{k6}	F'_{k1}	F'_{k2}	F'_{k3}	F'_{k4}	F'_{k5}	F'_{k6}	V_{kM}
1	1	1	1	1	1	0	0	0	0	0	0	$V_{dc} / 2$
1	1	1	1	1	0	1	0	0	0	0	0	$V_{dc} / 3$
1	1	1	0	0	0	1	1	0	0	0	0	$V_{dc} / 6$
1	1	1	0	0	0	1	1	1	0	0	0	0
1	1	0	0	0	0	1	1	1	1	0	0	$-V_{dc} / 6$
1	0	0	0	0	0	1	1	1	1	1	0	$-V_{dc} / 3$
0	0	0	0	0	0	1	1	1	1	1	1	$-V_{dc} / 2$

The voltage of the node k ($k = 1, 2, 3$) is relative to the middle point M and it is given by the following Eq. (2):

$$\begin{aligned}
 V_{kM} = & F_{k1}F_{k2}F_{k3}F_{k4}F_{k5}F_{k6}(U_{C1} + U_{C2} + U_{C3}) + F_{k1}F_{k2}F_{k3}F_{k4}F_{k5}(1 - F_{k6})(U_{C1} + U_{C2}) + \\
 & F_{k1}F_{k2}F_{k3}F_{k4}(1 - F_{k5})(1 - F_{k6})U_{C1} - F_{k1}'F_{k2}'F_{k3}'F_{k4}'F_{k5}'F_{k6}'(U_{C1} + U_{C2} + U_{C3}) - \\
 & F_{k1}'F_{k2}'F_{k3}'F_{k4}'F_{k5}'(U_{C1} + U_{C2})(1 - F_{k6}') - F_{k1}'F_{k2}'F_{k3}'F_{k4}'(1 - F_{k5}')U_{C1}
 \end{aligned} \quad (2)$$

To simplify Eq. (2), we define the connection functions F_k^b half-arm and $F_k^{'b}$ respectively associated to the half-arms of the top and bottom. To arm k, F_k^b and $F_k^{'b}$ are expressed using the switches connection functions as follows:

$$\begin{aligned} F_k^b &= F_{k1} F_{k2} F_{k3} F_{k4} F_{k5} F_{k6} \\ F_k^{'b} &= F_{k1}' F_{k2}' F_{k3}' F_{k4}' F_{k5}' F_{k6}' \end{aligned} \tag{3}$$

Namely that:

$$\begin{aligned} F_k^{b1} &= F_{k1} F_{k2} F_{k3} F_{k4} F_{k5} (1 - F_{k6}) \\ F_k^{'b1} &= F_{k1}' F_{k2}' F_{k3}' F_{k4}' F_{k5}' (1 - F_{k6}') \\ F_k^{b2} &= F_{k1} F_{k2} F_{k3} F_{k4} (1 - F_{k5}) (1 - F_{k6}) \\ F_k^{'b2} &= F_{k1}' F_{k2}' F_{k3}' F_{k4}' (1 - F_{k5}') (1 - F_{k6}') \end{aligned} \tag{4}$$

By introducing Eqs. (3) and (4) into Eq. (2):

$$\begin{aligned} V_{kM} &= F_k^b (U_{C1} + U_{C2} + U_{C3}) + F_k^{b1} (U_{C1} + U_{C2}) + F_k^{b2} U_{C1} \\ &- F_k^{'b} (U_{C1}' + U_{C2}' + U_{C3}') - F_k^{'b1} (U_{C1}' + U_{C2}') - F_k^{'b2} U_{C1}' \end{aligned} \tag{5}$$

Eq. (5) can be rewritten as follows:

$$\begin{aligned} V_{kM} &= (F_k^b + F_k^{b1} + F_k^{b2}) U_{C1} + (F_k^b + F_k^{b1}) U_{C2} + F_k^b U_{C3} \\ &- (F_k^{'b} + F_k^{'b1} + F_k^{'b2}) U_{C1}' + (F_k^{'b} + F_k^{'b1}) U_{C2}' + F_k^{'b} U_{C3}' \end{aligned} \tag{6}$$

The Eq. (6) proves that a seven-level inverter is a series of connection of six inverters at two levels. The voltages of a seven levels inverter are expressed using the connection functions of the switches as shown in Eq. (7).

$$\begin{aligned} \begin{bmatrix} V_{f1} \\ V_{f2} \\ V_{f3} \end{bmatrix} &= \frac{1}{3} \begin{bmatrix} 2 & -1 & -1 \\ -1 & 2 & -1 \\ -1 & -1 & 2 \end{bmatrix} \left\{ \begin{bmatrix} F_1^b + F_1^{b1} + F_1^{b2} \\ F_2^b + F_2^{b1} + F_2^{b2} \\ F_3^b + F_3^{b1} + F_3^{b2} \end{bmatrix} U_{C1} + \begin{bmatrix} F_1^b + F_1^{b1} \\ F_2^b + F_2^{b1} \\ F_3^b + F_3^{b1} \end{bmatrix} U_{C2} + \begin{bmatrix} F_1^b \\ F_2^b \\ F_3^b \end{bmatrix} U_{C3} \right. \\ &- \left. \begin{bmatrix} F_1^{'b} + F_1^{'b1} + F_1^{'b2} \\ F_2^{'b} + F_2^{'b1} + F_2^{'b2} \\ F_3^{'b} + F_3^{'b1} + F_3^{'b2} \end{bmatrix} U_{C1}' - \begin{bmatrix} F_1^{'b} + F_1^{'b1} \\ F_2^{'b} + F_2^{'b1} \\ F_3^{'b} + F_3^{'b1} \end{bmatrix} U_{C2}' - \begin{bmatrix} F_1^{'b} \\ F_2^{'b} \\ F_3^{'b} \end{bmatrix} U_{C3}' \right\} \end{aligned} \tag{7}$$

2.2. Control of strategies SPWM

The inverter is controlled by the Sinusoidal Pulse Width Modulation (SPWM) strategy [12-14]. The control signals of an inverter arm are determined by comparing the six carriers with three sin wave reference (Fig. 4).

This technique is characterized by two essential parameters:

- The modulation index, (m) is the ratio between the carrier frequency (f_p) and the frequency (f) of the sinusoidal reference.

- The modulation rate, (r) is the ratio between the carrier amplitude V_p and the amplitude V of the reference voltage.

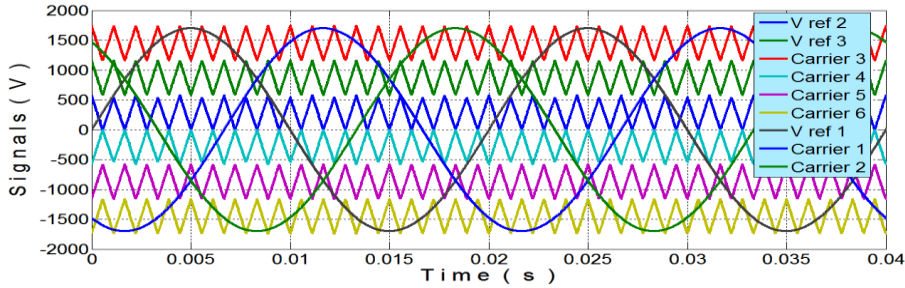


Fig. 4. Strategy phase opposition disposition (POD) SPWM inverter seven levels six carriers ($m = 18, r = 0.8$).

The algorithm of this strategy (Fig. 5) is based on the construction of the output voltage while respecting the midpoint M of an arm k . It is represented by the following Eqs. (8) and (9):

$$V_f = \sum_{i=1}^6 U_{f_{ki}} \quad , \text{ with } k = 1, 2, 3 \text{ and } j=1, 2, 3 \quad (8)$$

Knowing that intermediate voltages U_{ki} are calculated by:

$$\begin{cases} \text{if } V_{refk} \geq V_{pj} \text{ then } U_{kj} = U \text{ else } U_{kj} = 0 \text{ end if} \\ \text{if } V_{refk} \geq V_{p(j+3)} \text{ then } U_{k(j+3)} = 0 \text{ else } U_{k(j+3)} = -U \text{ end if} \end{cases} \quad (9)$$

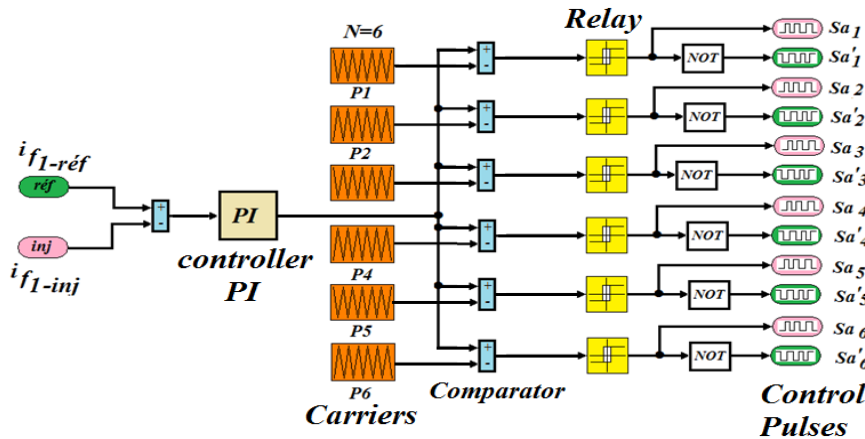


Fig. 5. Control algorithm PWM seven levels for APF (for phase 1).

The obtained simulation results (Fig. 6) show the seven voltage levels of V_{aM} (the voltage between the midpoint M and the inverter's first arm a), for $V_{dc} = 3400$ V and $C_1 = C_2 = C_3 = C_4 = C_5 = C_6 = 20$ mF.

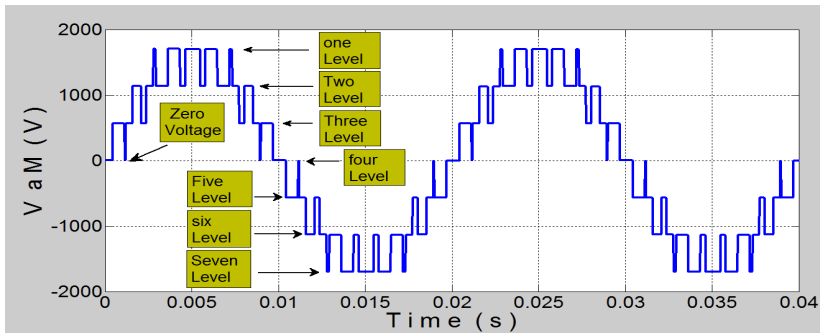


Fig. 6. Output voltage V_{aM} , of the seven level inverter ($m = 18, r = 0.8$).

3. Instantaneous Active and Reactive Power Theory (p-q)

This method [15,16] is the most commonly used, it has the advantage of choosing the disturbance as to compensate with the accuracy, the speed and the ease of implantation. The first step of this method is transforming the three phase (a, b, c) voltages/currents to two-phase α, β , using the Concordia Direct Transformation (CDT).

This method [17] consists on converting the fundamental component to an equivalent DC component and to harmonics AC components using low-pass filters (LPF) of the second order. We call (v_α, v_β) and (i_α, i_β) the orthogonal components of (α, β) . The instantaneous active and reactive power ($p-q$) can be expressed by the following system (10):

$$\begin{bmatrix} p \\ q \end{bmatrix} = \begin{bmatrix} v_\alpha & v_\beta \\ -v_\beta & v_\alpha \end{bmatrix} \begin{bmatrix} i_\alpha \\ i_\beta \end{bmatrix} \quad (10)$$

The powers p and q can be broken down by the system (11)

$$\begin{cases} p = \bar{p} + \tilde{p} \\ q = \bar{q} + \tilde{q} \end{cases} \quad (11)$$

\bar{p} is a part linked to the continuous active fundamental component of the current and \bar{q} is a part linked to the continuous reactive fundamental component of the current. \tilde{p} and \tilde{q} as fluctuating parts are linked to the sum of the harmonic components of the current and the voltage.

A low pass second order filter is used to separate the fundamental component from the interfering components. Two filters are needed, the first is to isolate the portion of the instantaneous active power, and the second is to isolate the portion of the instantaneous reactive power. Both filters are dimensioned taking account of the frequency decomposition of the powers in the two-phase coordinate system. The inverse powers of the Eq. (10) allows to establish the Eq. (12) currents i_α, i_β .

$$\begin{bmatrix} i_\alpha \\ i_\beta \end{bmatrix} = \frac{1}{v_\alpha^2 + v_\beta^2} \begin{bmatrix} v_\alpha & -v_\beta \\ v_\beta & v_\alpha \end{bmatrix} \begin{bmatrix} p \\ q \end{bmatrix} \quad (12)$$

Replacing the powers p and q by their DC and AC parts, the following system (13) is obtained:

$$\begin{bmatrix} i_\alpha \\ i_\beta \end{bmatrix} = \frac{1}{v_\alpha^2 + v_\beta^2} \begin{bmatrix} v_\alpha & -v_\beta \\ v_\beta & v_\alpha \end{bmatrix} \begin{bmatrix} \tilde{p} \\ 0 \end{bmatrix} + \frac{1}{v_\alpha^2 + v_\beta^2} \begin{bmatrix} v_\alpha & -v_\beta \\ v_\beta & v_\alpha \end{bmatrix} \begin{bmatrix} 0 \\ \tilde{q} \end{bmatrix} + \frac{1}{v_\alpha^2 + v_\beta^2} \begin{bmatrix} v_\alpha & -v_\beta \\ v_\beta & v_\alpha \end{bmatrix} \begin{bmatrix} \tilde{p} \\ \tilde{q} \end{bmatrix} \quad (13)$$

The calculation of harmonic currents in the two-phase reference (α, β) is finally given by the Eq. (14):

$$\begin{bmatrix} i_\alpha \\ i_\beta \end{bmatrix} = \frac{1}{v_\alpha^2 + v_\beta^2} \begin{bmatrix} v_\alpha & -v_\beta \\ v_\beta & v_\alpha \end{bmatrix} \begin{bmatrix} \tilde{p} \\ \tilde{q} \end{bmatrix} \quad (14)$$

Through the Concordia Reverse Transformation (CRT), the AC components of the powers allow us to deduce the three-phase harmonic currents. These currents represent disturbances and reference currents as shown in Eq. (15). They will be injected in phase opposition in the electrical network for suppressing harmonics.

$$\begin{bmatrix} i_a^* \\ i_b^* \\ i_c^* \end{bmatrix} = \sqrt{\frac{2}{3}} \cdot \begin{bmatrix} 1 & 0 \\ -\frac{1}{2} & \frac{\sqrt{3}}{2} \\ -\frac{1}{2} & -\frac{\sqrt{3}}{2} \end{bmatrix} \begin{bmatrix} \tilde{i}_\alpha \\ \tilde{i}_\beta \end{bmatrix} \quad (15)$$

Functional block of Fig. 7 explains and summarizes the reference currents calculation process by the method of instantaneous active and reactive power.

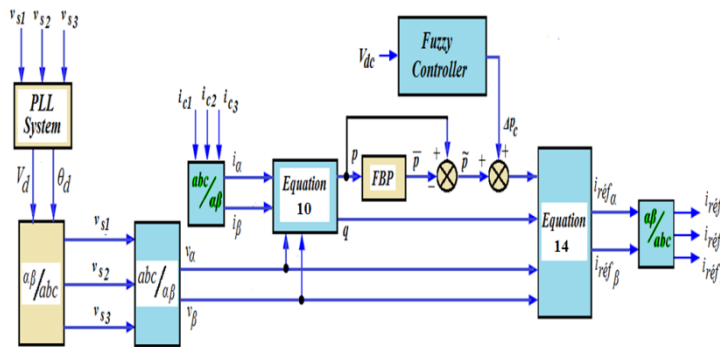


Fig. 7. Instantaneous active and reactive power algorithm.

4. DC Voltage Regulation

The voltage of the DC bus filter is held constant by a fuzzy controller. This latter keeps the voltage V_{dc} in a fixed value called reference voltage V_{dc-ref} (V_{dc}^*). The block diagram of the fuzzy control technique is shown in Fig. 8 below. The adjustment method consists [18-20] of ensuring the inputs of the fuzzy controller. The error $e(t)$ between the value of the voltage V_{dc} of the capacitor with its reference V_{dc}^* is considered as a first input variable, while its derivative is considered as a second input variable $\Delta e(k)$. The instantaneous error $e(k)$ between V_{dc} and its reference V_{dc}^* , is given by Eq. (16):

$$e(k) = v_{dc}^*(k) - v_{dc}(k) \quad (16)$$

The change of the error can be calculated by Eq. (17):

$$\Delta e(k) = e(k) - e(k - 1) \tag{17}$$

The output of the fuzzy logic controller system is the variation of the maximum current $\mu(k)$. The Product block's outputs $P(k)$ is the multiplying result of the DC voltage error $e(k)$ and the maximum output current of the Fuzzy Logic Controller (FLC), obtained according to following Eq. (18):

$$P(k) = \mu(k) \cdot \Delta e(k) \tag{18}$$

The fuzzy rules are summarized in Table 2. The membership functions of the fuzzy logic controllers are shown in Fig. 9.

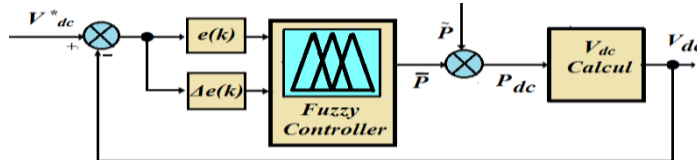


Fig. 8. DC voltage fuzzy control of SAPF.

Table 2. Rule base table.

Derived of error $\Delta e(k)$	N	Z	P
N	B	M	B
Z	B	S	B
P	B	M	B

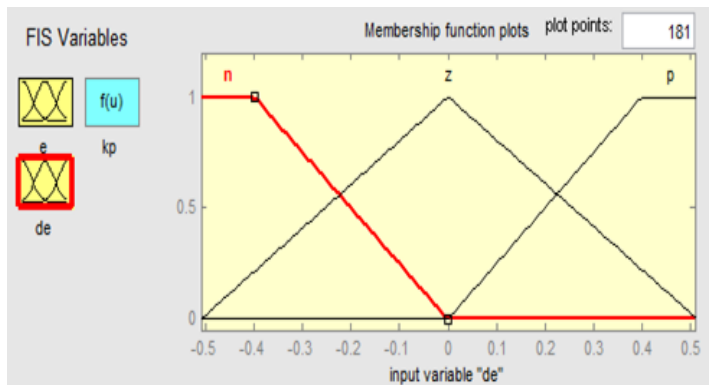


Fig. 9. Input membership function.

5.Simulation and Interpretation

The simulation was performed to confirm the theoretical study in static mode and for verifying dynamic performances of (A P F). To assess the effectiveness so four approach, based on the method of instantaneous power ($p-q$) calculation, we performed robustness tests by changing the load value and the reference V_{dc} . Figure 10 shows the current wave form before compensation. Clearly it is distorted, and this is because of the harmonics. Spectral analysis of such wave form is shown in Fig. 11. This shows the presence of $6k \pm 1$ order harmonics and total distortion of 17.19%.

That exceeds from afar international norms. After compensation in the time of the insertion of the shunt active power filter (SAPF) with the network (Fig. 12), we notice that the form of current is improved and it recovers the sin wave. The total distortion is 2.9 %, so considerably better than before compensation. Parameters used in simulation are as follows in Table 3.

Spectral analysis gives a fundamental line corresponding to the frequency of 50Hz, so it's clean in term of power quality (Fig. 13). Figures 14 and 15 show the control of the direct voltage of APF, before and after insertion of the fuzzy logic controller. When connecting the APF with the network, the DC bus voltage increases to 3400 V, following the reference voltage V_{dc-ref} .

Table 3. Parameters used in simulation.

Electrical Device	Parameters
Power Source	RMS Voltage 1.2kV/2.1 kV, Frequency $f=50$ Hz, $R_s = 0.2 \Omega$, $L_s = 0.001$ mH
Filter RL	$L_f = 45$ mH, $R_f = 0.05 \Omega$, $L_c = 5$ mH, $R_c = 10 \Omega$
Load	3 phase rectifier bridge(PD3)IGBT initially powers, R-L load then added to each moment in parallel resistive load
Active Power Filter(A P F)	Based on an inverter, IGBT has seven by SPWM six Carriers, Storage capacity: $C = 20$ mF, Capacitor initial voltage:500 V, Reference voltage $V_{dc-ref} = 3400$ V.

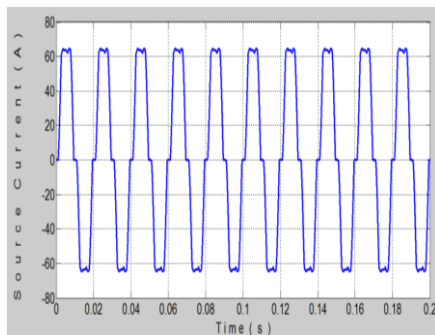


Fig. 10. Source current without shunt APF.

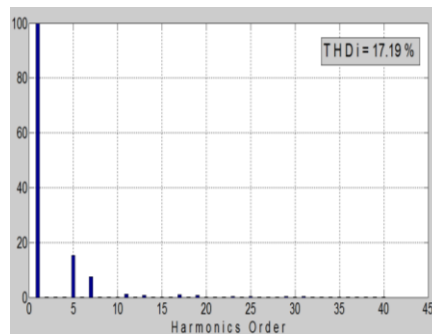


Fig. 11. Source current spectrum shunt APF.

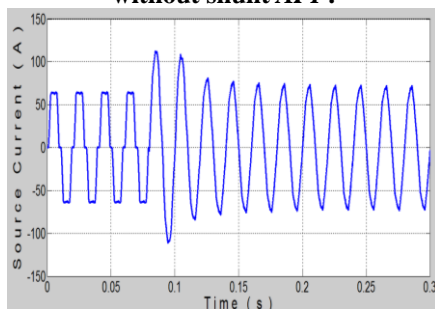


Fig. 12. Source current before and after compensation.

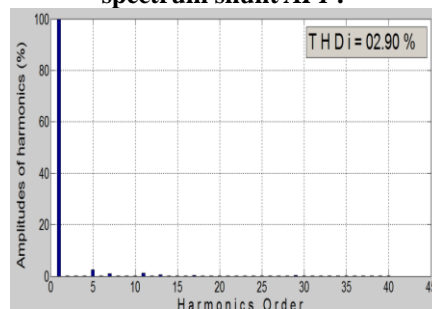


Fig. 13. Source current spectrum with shunt APF.

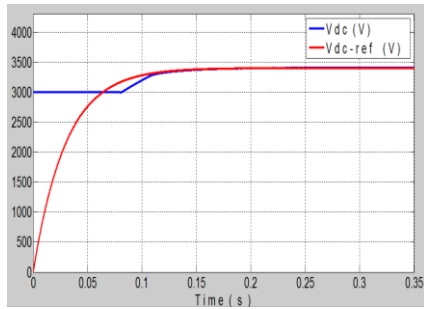


Fig. 14. DC side capacitor voltages V_{dc} .

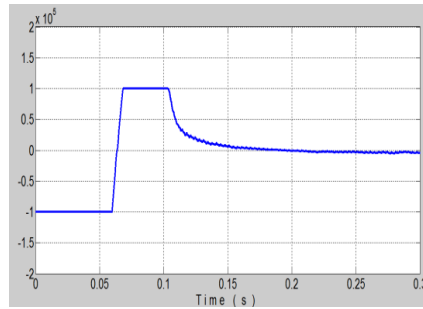


Fig. 15. Response of the fuzzy controller before and after compensation.

The fuzzy logic controller starts from 0.08s and keeps the stability of the voltage V_{DC} to the reference value. At that time the filter injects harmonic currents in the network, as shown in Figs. 16 and 17 for the first phase.

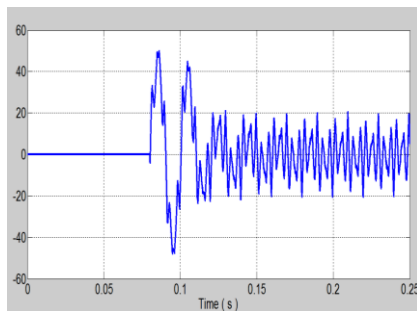


Fig. 16. Injected current I_{ha} (A).

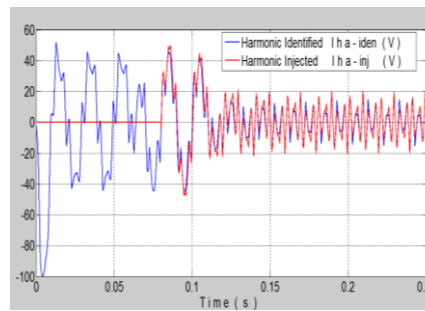


Fig. 17. Synchronization between identified and injected harmonics.

In fact, a marked superposition between the identified and the injected current, allows to obtain a purely sinusoidal current source corresponding to the power frequency 50 Hz (Fig. 18). This latter is in phase with the supply voltage. As a result, it induces a unity power factor (Fig. 19).

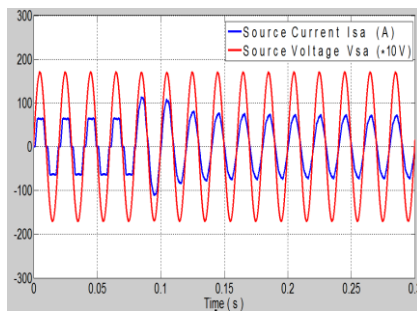


Fig. 18. Source current and source voltage V_{sa} before and after compensation.

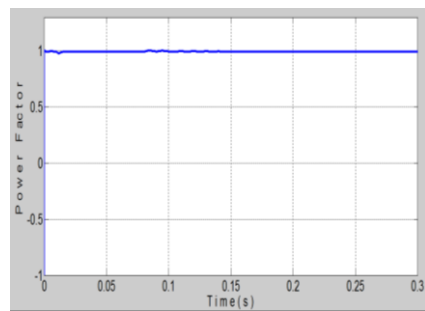


Fig. 19. Power Factor (PF).

It is found from Figs. 20, 21, 22, 23 and 24, that the fuzzy logic controller keeps the stability of the DC voltage. As a result, the V_{dc} follows correctly the 3400V reference voltage despite the variations experienced by the load in the time interval [0.2 s-0.5 s]. Indeed the amplitude of the current source and that of harmonic injected increases with the inrush current caused by the increased load.

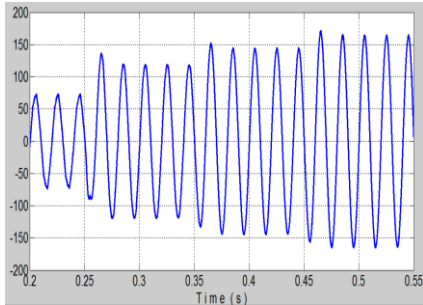


Fig. 20. Source current with step change in load (Between $t_1= 0.2$ s - $t_2= 0.5$ s).

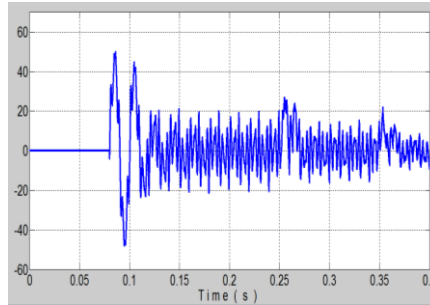


Fig. 21. Injected current I_{ha} (A) with step change in load.

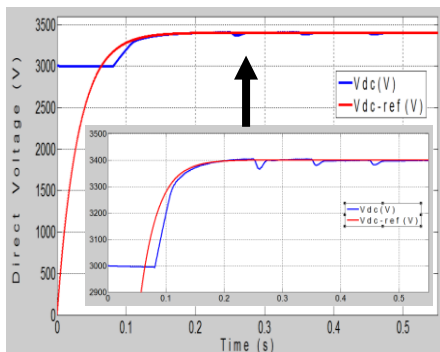


Fig. 22. DC side capacitor voltage with step change in load (Between $t_1= 0.2$ s - $t_2= 0.5$ s).

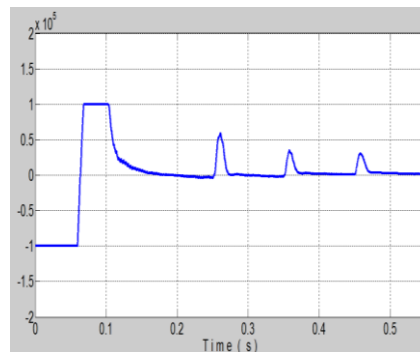


Fig. 23. Response of fuzzy controller before and after compensation during the load change.

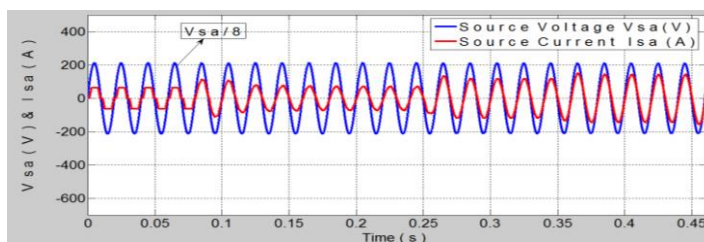


Fig. 24. Source current and voltage before and after compensation with step change in load (between $t_1= 0.2$ s- $t_2= 0.5$ s).

Starting at time $t = 0.08$ s (Fig. 25), the fuzzy logic controller is always maintaining the synchronization between the identified current and the injected current even during load change. We deduce according to Fig. 26, that the DC bus

voltage always follows the reference for other values such as 3000V, 3400V, 4000 V and 4300 V.

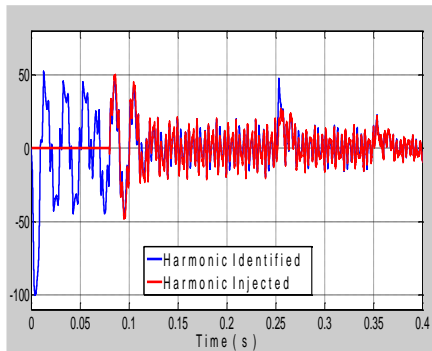


Fig. 25. Synchronization identified and injected harmonic currents during the variation of the load.

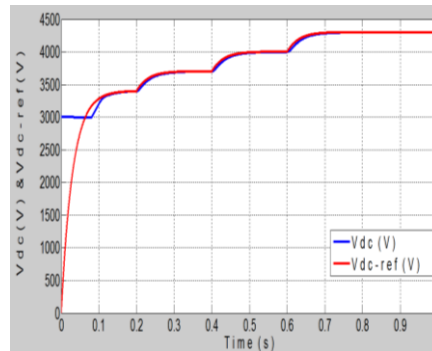


Fig. 26. V_{dc} follows the reference V_{dc-ref} .

Figures 27 and 28 clearly illustrate the robustness of the APF, confirm again the stability and the efficiency that provides the fuzzy logic controller, despite the disruptions created by both of the change of the load and the passage of a constant value of V_{dc} to another. Hence, we find that the source current changes with the load but not with the DC bus voltage.

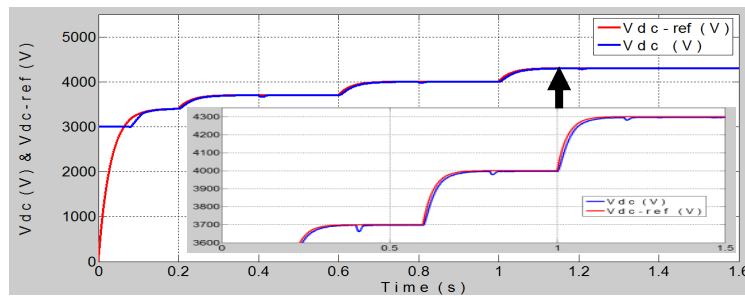


Fig. 27. V_{dc} follows the reference V_{dc-ref} with the load variation between 0.2s-1.4s.

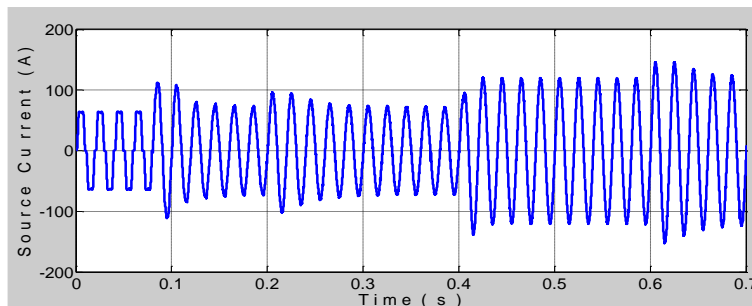


Fig. 28. Current wave form during the variation V_{dc} and the load, between 0.2s-0.7s.

6. Conclusions

The Clearance of harmonic currents in an electrical network may be possible with the development of multilevel active filter based of new components with forced commutation as the *GTO* thyristor, and *IGBT*. This work is devoted to the study of the active filter parallel to seven levels based on a fuzzy regulator. After a brief theoretical synthesis of to the modelling and the *SPWM* control of the seven levels inverter and of the theory of active and reactive power $p-q$. The results of numerical simulation have justified the use (feasibility and reliability) of the multi-level filter in the contribution to the mitigation of harmonics that affect the correct functioning of the network. Using the identification method of harmonics by the principle of calculating the instantaneous active and reactive power, the *FAP* provides high efficiency and accuracy. Indeed, a significant superposition between the injected and identified current has provided purely sinusoidal currents with unity power factor. The multilevel *FAP* remains the most applied filter in the high voltage range and high power, due to its great performance during the filtering operation, and this, despite the load changes and instability of the *DC* bus.

References

1. Li, L.; Czarkowski, D.; Liu, Y.; and Pillay, P. (1998). Multilevel selective harmonic elimination PWM technique in series-connected voltage inverters. *Proceedings of the 1998 IEEE Industry Applications Conference. Thirty-Third IAS Annual Meeting* . Missouri, United States of America, 1454-1461.
2. Tehrani, K.A. (2010). *Design, synthesis and application of a robust new control by fractional PID for multi-level inverters*. Ph.D. Thesis. National School of Electricity and Mechanics, National Polytechnic Institute, Lorraine, France.
3. Vahedi, H.; Al-Haddad, K. (2016). Real-time implementation of a seven-level packed U-Cell inverter with a low-switching-frequency voltage regulator. *IEEE Transactions on Power Electronics*, 31(8), 5967-5973.
4. Chennai, S. (2016). Efficient control scheme for five-level shunt active power filter to enhance the power quality. *Electrical Engineering, Electronics, Automation (EEA)*, 64(4).
5. Manjrekar; M.D., Steimer, P.K.; and Lipo, T.A. (2000). Hybrid multilevel power conversion system: a competitive solution for high power applications. *IEEE Transactions on Industry Applications*, 36(3), 834-841.
6. Diga, S.-M.; Ruşinaru, D.; and Grigorescu, A.C. (2006). Aspects concernant la limitation des effets de la circulation des harmoniques dans les reseaux de distribution. *Annals of the University of Craiova, Electrical Engineering, Series 30*, 282-287.
7. Abeslam, D.O. (2005). *Neuromimétriques techniques for control in power systems: Application to shunt active filter in low voltage electrical networks*. Ph.D. Thesis, University of Haute Alsace, Mulhouse, France.
8. Saadate, S. (1995). *G-T-O Thyristor high power fully controllable switch for electric traction analysis and treatment induced disturbances in the power network by static converters AC/DC*. Habilitation research, University of Lorraine, Nancy, France.

9. Lott, C. (1995). *Shunt active power filtering current harmonics on industrial networks theoretical study and realization of a model GTO*. Ph.D. Thesis. University of Lorraine, Nancy, France.
10. Barkat, S. (2008). *Modeling and control of a seven-level inverter LED floating application for driving asynchronous machine*. Ph.D. Thesis. National Polytechnic School (ENP), Algeria, Africa.
11. Lalili, D.; Lourci, N.; Berkouk, E.M.; Boudjema, F.; Petzoldt, J.; and Dali, M.Y. (2006). Simplified space vector pulse width modulation algorithm for five-level diode clamping inverter. *Proceedings of the International Symposium on Power Electronics, Electrical Drives, Automation and Motion (SPEEDAM06)*, Taormina, Italy, 1349-1354.
12. Vasiladiotis, M. (2009). *Analysis, implementation and experimental evaluation of control systems for a modular multilevel converter*. Master Thesis. Department of Electrical Engineering, Royal Institute of Technology, Stockholm, Sweden.
13. Djebbar, M.S.; Benalla, H.; and Soufi, Y. (2013). Cascade rectifiers and multi levels applied to the improvement of the quality of electric energy. *Proceedings of the Eighth International Conference and Exhibition on Ecological Vehicles and Renewable Energies (EVER)*, Monaco, France, 1-7.
14. Natarajan, P.; and Kaliannan, P. (2016). Comparative analysis of symmetric and asymmetric reduced switch MLI topologies using unipolar pulse width modulation strategies. *IET Power Electronics*, 9(15), 2808-2823.
15. Akagi, H.; Kanazawa, Y.; and Nabae, A. (1983). Generalized theory of the instantaneous reactive power in three-phase circuits. *Proceedings of the International Power Electronics Conference*. Tokyo, Japan, 1375-1386.
16. Akagi, H. ; Kanazawa, Y.; and Nabae, A. (1984). Instantaneous reactive power compensators comprising switching devices without energy storage components. *IEEE Transactions on Industry Applications*, IA-20(3), 625-630.
17. Nabae, A.; Takahashi, I.; and Akagi, H. (1981). New neutral-point-clamped PWM inverter. *IEEE Transactions on Industry Applications*, IA-17(5), 518- 523.
18. Lokman, H.; Moghavvemi, M.; and Mohamed, H.A.F. (2010). Takagi-Sugeno. Fuzzy gains scheduled PI controller for enhancement of power system stability. *American Journal of Applied Sciences*, 7(1), 145-152.
19. Boukadoum, A.; and Bahi, T. (2014). Harmonic current suppression by shunt active power filter using fuzzy logic controller. *Journal of Theoretical and Applied Information Technology*, 68(3), 651-656.
20. Hamadi, A., Al-Haddad, K.; Lagace, P.J.; and Chandra, A. (2004). Indirect current control techniques of three phases APF using fuzzy logic and proportional integral controller. *Proceedings of the 11th IEEE International Conference on Harmonics and Quality of Power*. New York, United States of America, 362-367.